Pak. j. sci. ind. res. Ser. A: phys. sci. 2026 **69A**(2) 55-65 https://doi.org/10.52763/PJSIR.PHYS.SCI.69.2.2026.55.65

Effect of Vacuum Induction Melting and Vacuum Arc Remelting Treatment on Inclusion Level and Mechanical Properties of AISI H13 Tool Steel

Muhammad Adeel Rauf[a], Muhammad Kamran Bhatti[a] and Zubia Anwer[b]*
[a]Department of Materials Engineering, NEDUET, University Road, Karachi, Pakistan
[b]Department of Metallurgy Engineering, NEDUET, University Road, Karachi, Pakistan

(received January 11, 2024; revised November 3, 2025; accepted November 4, 2025)

Abstract. AISI H13 steel grade was produced using vacuum induction melting (VIM) followed by vacuum arc remelting (VAR), instead of the traditional Ingot casting method. Samples were taken from both ingots, namely the conventional and VAR-treated ones. These samples were then forged with the same reduction ratio. The forged samples were tested for non-metallic inclusions. Additionally, gas content analysis was performed using an Oxygen/Nitrogen/Hydrogen detector (OHN-detector) to measure the levels of hydrogen, nitrogen and oxygen in the samples. Mechanical testing was conducted and a comparative analysis was performed to assess how both production routes affected the properties of H13 tool steel. Thermodynamic calculations revealed that the VAR-treated ingots had lower inclusion levels, with a 16% reduction in (Mn, Fe) S, a 25% reduction in sulphides and complete removal of silicates and oxide-based inclusions. These samples also exhibited improved mechanical properties, with a 39.48% increase in impact strength and a 12.11% increase in tensile strength compared to conventionally cast H13. The thermodynamic analysis indicated the presence of MnS and SiO_2, along with the trapping of hydrogen and nitrogen. A high non-metallic inclusion index (NMI), combined with hydrogen and nitrogen entrapment, is the primary cause of the reduced mechanical properties.

Keywords: H13 tool steel, vacuum induction melting, vacuum arc remelting, non-metallic inclusion index, mechanical properties, Factsage

Introduction

AISI-H13 finds itself among the air-hardening hot work tool steels known for its excellent hardenability, wear resistance and high tensile strength (Li *et al*., 2020; Bahrami *et al*., 2005). This steel group offers ease to the extent that it can be hardened in air and oil (Avner, 1974). The combination of high strength along good wear resistance is due to a phenomenon known as secondary hardening that takes place during tempering at a certain temperature range (Ning *et al*., 2017; Qamar *et al*., 2007). The H13 is known to possess considerable resistance to wear, good strength at elevated temperatures and toughness (Guanghua *et al*., 2010; Davis, 1995; Dorsch *et al.*, 1995). This is the reason why it is mostly utilized as a die material for forging, extrusion and other related die-forming processes taking place at elevated temperatures (Mertens *et al*., 2016; Benedyk, 2008). The production of H13 through the conventional route in most industries involves melting in an electric arc furnace, achieving chemistry in a ladle furnace and then casting in ingots. Only a few industries perform vacuum degassing before casting. Even then, the inclusion level of steel is considerable enough to cause problems not only in service conditions but also during material testing when mechanical properties are found to be in the lower range (EEIMVR-UFF, 2018; Song *et al*., 2011; Tomita, 1995; Nordgren and Melander, 1989). In addition, the melting carried out in VAR offers a controlled mode of solidification and processing can take place under varying conditions of atmospheres and pressure conditions it provides supreme material quality (Campbell, 2023). Furthermore, melting in VAR eradicates the need to cast in an open environment and other factors such as ladle erosion and the use of casting powder. This in turn favors the casting process in a way that chances of entrapment of exogenous inclusions are mitigated to a greater extent.

Therefore, it is necessary to mitigate the level of inclusion to eradicate problems associated with the presence of non-metallic inclusions. This approach involves producing H13 under extremely low pressure in a vacuum induction furnace and then further refining it through vacuum arc remelting. This study is based on

*Author for correspondence; E-mail: zubia@neduet.edu.pk

a specific purpose *i.e*., information on resultant phases and inclusions by applying computational thermodynamics for H-13 alloy and the mechanical performance of alloy in both conventional and VAR casting conditions. The present study is novel due to thermodynamic prediction for the existing inclusions.

Materials and Methods

The steel scrap used in the vacuum induction furnace is in billets form having a cross-section of 75×75. The normal length is one meter. (Haupt *et al*., 2017; Pauliuk *et al*., 2013; Ma *et al*., 2009). The typical ferroalloys are used for alloy addition *i.e*., ferrochrome, ferromolybdenum, silicon-manganese and ferro-vanadium etc. The sample of 10×10×2 mm^3 was used for metallographic analysis. A hot-mounted sample has been ground progressively up to 1000 grid emery paper and then polished using alumina suspensions and cleaned ultrasonically in ethanol.

Vacuum induction melting. The crucible is supplemented with a vacuum system inside a steel shell backed up by refractory material as an insulating medium. The copper coils are cooled by access to water that flows through the tube assembly. The rest of the principle is based on the mechanism of induced current. The current in the copper coils, which serve as a primary coil creates magnetic flux around the steel which upon passing the scrap, which acts as a secondary coil, induces current in it. The metal melts due to the heat generated by the resistance that metal provides to the flow of current. The eradication of unwanted trace constituents like antimony, bismuth and copper, with the help of an induction furnace supplemented with a vacuum is of paramount importance (Van Ende *et al*., 2013; Deo and Boom, 1993).

The VIM ingot is then further refined through vacuum arc remelting to further enhance the cleanliness level of the steel. This approach serves to further mitigate the level of impurity and can significantly enhance the performance of the VIM+VAR-made AISI H-13 as compared to the traditional H13. Although the standard composition remains the same, the cleanliness level of the former is found to be marginally minimized due to vacuum practice (Wu *et al*., 2022). The FactSage was used to analyze the resultant inclusion phases between 1000 °C-1800 °C.

VAR. The vacuum arc remelting treatment is strictly carried out in an evacuated, low-pressure environment. The crucible used is water-cooled and made of copper. It is the interface between the electrode tip and the molten pool, at the top of the ingot where the refining takes place. The mode of solidification here is the top towards the bottom. The resulting output is a material with excellent metallurgical properties, no center cavities, freckle region and complete uniformity of the composition throughout the ingot and most of this boils down to the fact that solidification took place in a controlled manner. A drastic reduction in NMIs is now possible as the vacuum level reaches 0.01 torr at an elevated temperature of 1710 °C. (Campbell, 2023).

Forging. To ensure that the comparison is made at an equal level, both conventional and VAR-treated H13 ingots are forged by keeping the reduction ratio the same. The samples were reheated to the hot working temperature of 1150 ºC and then forged with a 3-ton hammer to produce the desired round bars.

The input material for forging was drawn from both ingots separately having the dimensions of 75×100 mm bars. The round bars forged were of 18 mm diameter and the reduction ratio was 7.

Machining. The deformed round bars are then annealed so that tensile and impact samples can be drawn with ease. The usual method followed for drawing tensile specimens was ASTM A370. The entire dimensions followed this standard.

Heat treatment. Since H13 is a hot work die steel, it is used in hardened and tempered conditions in service operations (Totten, 2006; Wayman, 1964). Therefore, properties were to be examined in the same condition.

The material was subsequently subjected to annealing treatment in a heat treatment furnace Carbolyte, RHF 16-8 (UK) to get the desired microstructure. The material was heated to 1050 °C for austenitizing for 15 mins. Sufficient time is crucial to allow proper homogenization and diffusion. Inadequate time would lead to incomplete austenite transformation and thus martensite along with the ferrite phase (Medvedeva *et al*., 2009; Qamar *et al*., 2007). The soaking is followed by air cooling since it can be hardened in air as well as oil (Medvedeva *et al*., 2009). Therefore, samples were hardened and tempered at the same parameters to obtain service condition properties. For H13, a single tempering cycle is not enough. Mostly H13 is double or triple-tempered to obtain the best combination of both strength and toughness (Mao *et al*., 2016). Since it is air-hardening steel, preference could be given to air cooling rather than oil quenching to have a comparatively tougher martensite (Zhu *et al*., 2020). In this case, double tempering was done after hardening through air cooling. Tempering should be started immediately as soon as the temperature of the material reaches 50 to 70 °C or else, cracking could result (Smoljan, 2009; Mebarki *et al*., 2004).

1st tempering was performed at 600 °C for 2 h. Since, lower tempering temperatures *i.e*., 560 °C-580 °C result in temper embrittlement (Samuel, 1983). The 2nd tempering was performed immediately after 1st tempering at a temperature of 620° C for 2 h (Ferrari *et al*., 2013; Zhong, 2007; Huang and Liu, 1996; Samuel, 1983). Both tempering cycles were followed by air cooling as in Fig. 1.

Tensile testing. Tensile properties were analyzed using tensile testing ASTM A370. The tensile testing was performed for both conventionally treated and VAR-treated samples in hardened and tempered conditions. The ASTM E-8 was used to prepare standard samples for tensile testing using the ultimate tensile testing machine Instron (60 MT) having UK origin. The measurements are made around the reduced section of the gauge length. The elongation measurement is used to calculate the engineering strain, ε, using the following equation.

$$\varepsilon = L\text{-}L_0/L_0$$

Where L_0 is the initial gage length and L is the reduced gage length. Engineering stress, σ is calculated using the following equation:

$$\sigma_e = F/A_0$$

For calculating the percent reduction in the final sample, the following equation is used

$$R = A_0 – Af/A_0$$

Where A_0 is the initial cross-sectional area and Af is the final reduced cross-sectional area. The percent elongation is calculated as

$$EL = L\text{-}L_0/L_0$$

Impact testing. The room temperature impact properties for conventionally treated and VAR-treated material after hardening and tempering were analyzed using an impact testing machine DT&T of Korean origin. The ASTM A370 was followed as the standard testing procedure whereas, ASTM E23-24 was used for making Charpy V-notch specimens having a cross-sectional area of 10 mm^2, having a length of 55 mm. The V-notch and the sample geometry are shown in Fig. 2. (International, 2022)

Hardness testing. The hardness test is done using the Rockwell hardness tester, using the C scale. Like the rest of the study, hardness is also compared for both the conventionally treated sample and VAR treated sample in hardened and tempered conditions. The standard procedure followed for this testing is ASTM E18.

Testing and characterization. ***Optical emission spectroscopy.*** The chemical analysis for steel ingots was performed using ASTM E-1009 as in Table 1.

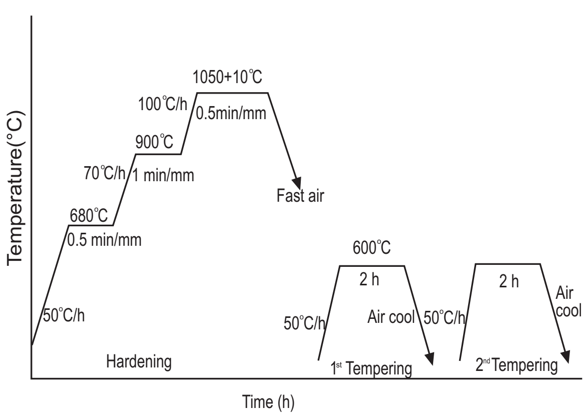

Fig. 1. Heat treatment cycles for both hardening and tempering of the alloy.

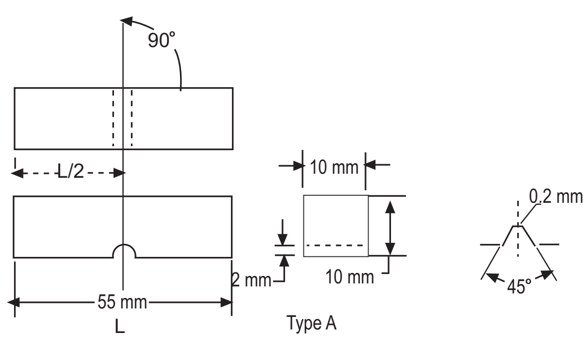

Fig. 2. Dimensions of charpy impact sample as ASTM E 23-24.

Table 1. Chemical composition of H13 alloy (wt-%)

C	Si	Mn	P	S	Cr	Mo	V	Fe
0.34	1	0.3	0.021	0.021	5.50	1.45	0.9	Bal

Rapid analyzer (oxygen/nitrogen/hydrogen detector). The oxygen/nitrogen/hydrogen detector named Eltra (Germany) was utilized for detecting the gas content of H13 that was previously produced through conventional ingot casting and one that is produced through the VAR process. The standard followed is ASTM E-1019.

***Optical microscopy*.** The optical microscope Olympus (Korea) was used for both microstructure and inclusion analysis. The quality of the alloy in both conventional and VAR-treated conditions was under investigation. Moreover, the extent of the heat treatment procedure was confirmed using microstructure analysis. The non-metallic inclusion indexing (NMI index) has been performed as a polished condition using ASTM E-3 for sample preparation and ASTM E-45 for indexing. Whereas, the metallographic sequence *i.e.*, grinding up to 1000 grid emery, polishing in colloidal alumina and etching in 5% Nital was followed by microscopic examination.

Thermodynamic study. Thermodynamic calculations were carried out using both chemical composition and the temperature range of 1000 °C to 1800 °C. The obtained results were about the chemical composition of steel and inclusions at process temperature. The thermodynamic study was performed with FactSage 7.2. Bale discussed a general description of its databases and modules (Bale *et al*., 2009). The FToxid and FSstel databases were used with the FactSage Equilib module. The steel-inclusions equilibria were calculated (Bielefeldt and Vilela, 2010).

Results and Discussions

In ingot casting, even though vacuum degassing has already been done before taking the ladle to the ingot casting station, inclusion could arise due to the interaction of melt with the mold assembly (Ragnarsson, 2010; Waudby, 1973). The laddle nozzle could be a source of exogenous inclusions. Moreover, during the transfer of the ladle to the casting station, the metal gets oxidized again which leads to small-size inclusion formation. The same phenomenon also occurs inside the mold (Ragnarsson, 2010). Moreover, the excessive usage of casting powder could also aid in the formation of inclusions (Ragnarsson, 2010; Ragnarsson and Sichen, 2010). Silicates are a kind of inclusion that could be present as a result of silicon in melt reacting with the oxygen of the atmosphere and due to erosion of the refractory lining. These all factors can compromise the quality of steel (Waudby, 1973). The limited solubility of sulfur in iron may also be the cause of sulfide inclusions (Huang *et al*., 2019). Moreover, the moisture content in mold or the grating system may also be the source of oxygen and then oxide-based inclusions (Huang and Liu, 1996). Therefore, the presence of inclusions in ingot cast steels is a problem that could only be mitigated to a limited extent (in open-casting processes) because of operational limitations.

Oxygen/nitrogen/hydrogen content. Table 2 shows the oxygen, nitrogen and hydrogen content for both conventional treated and VAR treated ingots.

Table 2. The comparison of oxygen/nitrogen/hydrogen content

Sample	Hydrogen (ppm)	Nitrogen (ppm)	Oxygen (ppm)
Conventionally cast	1.50	249	26
VAR treated	0.90	25	1.7

Table 3. Inclusion content of conventional treated ingot

Sample	Analysis of conventional ingot							
	Sulfides (A)		Alumina (B)		Silicates (C)		Oxides (D)	
	Thin	Heavy	Thin	Heavy	Thin	Heavy	Thin	Heavy
Max limit	≤ 0.5	≤ 0.5	≤ 1.0	≤ 0.5	≤ 1.0	≤ 0.5	≤ 1.0	≤ 0.5
Conv. treated	2.0	1.0	--	--	1.0	--	2.0	1.5

Table 4. Inclusion content of VAR-treated ingot

Analysis of VAR-treated ingots							
Sulfide (A)		Alumina (B)		Silicates (C)		Oxides (D)	
Thin	Heavy	Thin	Heavy	Thin	Heavy	Thin	Heavy
≤ 0.5	≤ 0.5	≤ 1.0	≤ 0.5	≤ 1.0	≤ 0.5	≤ 1.0	≤ 0.5
--	--	--	--	--	--	0.5	0.5

Non-metallic inclusion index. The inclusions *i.e.*, sulfides, oxides, silicates and alumina were analyzed using the standard method as discussed in section 2.3.3. The NMI index for each conventionally treated and VAR treated are summarized in Tables 3 and 4 respectively. The microscopic analysis in a polished condition for both conventionally treated and VAR-treated steel is shown in Fig. 3(a-e) and Fig. 4 respectively.

Tempering of this grade is necessary in order to obtain the maximum benefit of increment in hardness which result because of a process known as secondary hardening in which precipitates of chromium, molybdenum and vanadium carbides form and result in hardness and wear resistance of the tool steel (Olson *et al*., 2013; PAN *et al*., 2009).

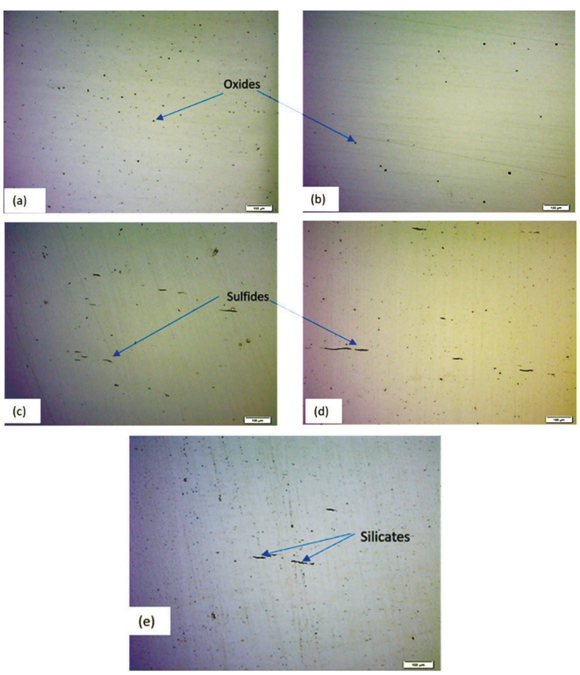

Fig. 3. Micrographs of conventional treated samples in a polished condition taken at 100x. Figure (**a**) and Figure (**b**) show thin & thick oxides respectively. Figure (**c**) and Figure (**d**) show thin and thick sulphides respectively. Figure (**e**) shows thin silicates.

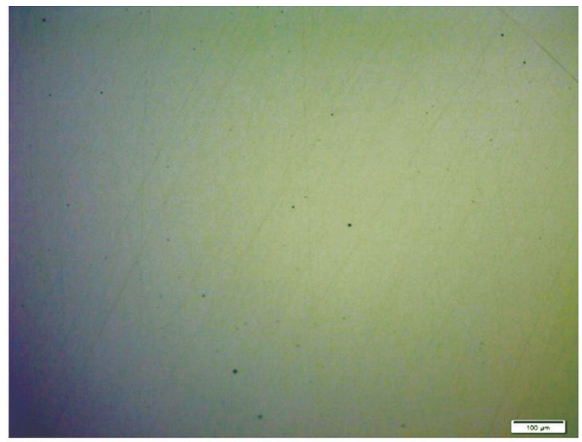

Fig. 4. Micrograph of VAR treated sample.

Hardness. The Vicker hardness testing has been performed using scale C for both conventionally and VAR treated samples as shown in Table 5.

The Tables 6 and 7 represents tensile and impact properties in hardened and tempered condition for both alloys *i.e*., conventional and VAR treated respectively.

Table 5. Rockwell hardness values in hardened and tempered conditions

Sample condition	Microstructure	Hardness (HRC)
Hardened and tempered (Conventional treated)	Tempered martensite	46±1
Hardened and tempered (VAR treated)	Tempered martensite	47±1

Mechanical properties

Table 6. Mechanical properties for conventionally treated ingots after tensile and impact testing

Sample	Yield strength (MPa)	Tensile strength (MPa)	Elongation (50%-gauge length) (%)	Reduction toughness (J)	Impact
1	1271	1352	11	54	23
2	1218	1345	12	56	23
3	1196	1365	13	51	25
Average	1228.3	1354	12	53.6	23.6

Conventionally cast

Table 7. Mechanical properties for VAR treated ingots after tensile and impact testing

Sample	Yield strength (MPa)	Tensile strength (MPa)	Elongation (50%-gauge length)	Reduction (%)	Impact toughness (J)
1	1369	1514	10	63	38
2	1432	1516	10	56	41
3	1477	1592	08	58	38
Average	1426	1540.6	9.3	59	39

VAR treated

Viewing the mechanical properties (Table 6 and 7) and comparing these with the level of inclusion, it is evident that the increased properties of VAR-treated H13 are due to the cleansing level of steel as shown in Fig. 6 a-e. This is because inclusions negatively affect mechanical properties. They can create stress concentration points around which a crack is more likely prone to initiate once subjected to an external load (Peaslee *et al*., 2011). Moreover, exogenous inclusions

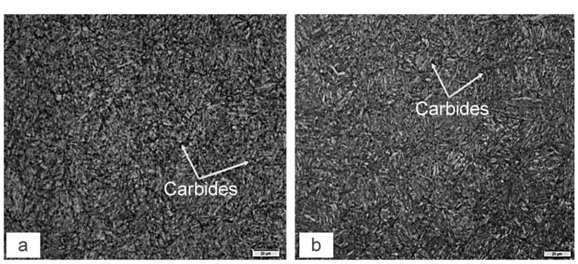

Fig. 5. Microstructure revealed at 100X using 5% Nital in hardened and tempered conditions; (a) Conventionally treated and (b) VAR treated.

that are larger are harmful to the toughness and notch sensitivity of die steel. The higher the level of inclusions in molten steel worse the end result after solidification since inclusions serve as a nucleation site for other inclusions and hydrogen trapping (Peaslee *et al*., 2011; Thornton, 1971). Also due to the absence of sulfides, chances of inter-granular cracking are minimized since sulfide inclusions are known to cause inter-granular cracking during hot working (Maciejewski, 2015). A higher inclusion index would result in a further decline in mechanical properties. On the other hand, VAR-treated samples, because of their negligible inclusion content show better mechanical properties and toughness levels compared to conventionally cast ones. The toughness level of VAR-treated steel *i.e*., 39 Joules is better than conventional treated *i.e*., 23.6 Joules and this is due to the absence of sulfide inclusions which, if present, reduce the impact toughness of the steel (Cyril *et al*., 2009).

Prediction of inclusions during cooling of liquid steel. The NMI index for both conventionally treated and VAR treated alloy has been discussed in Table 3, 4 and the associated microscopic results are shown in Figure 3 and 4 respectively.

Based on the composition shows in section 2.3.1, the thermodynamic calculations were made as shown in Fig. 7 and 8 for conventional treated and VAR treated steels respectively. The analysis was made at temperature range of 1000 °C-1800 °C. The sulfide, silicate and oxide-based inclusions in molten steel were form and grow during cooling of steel from the ladle treatment. The higher amount of inclusions in conventional ingot casting are due to continuous temperature drop from ladle furnace to caster (Ghosh, 2009) as shown in Table 3 and Fig. 7. However, in case of vacuum treatment, only a little amount of oxide inclusions formed below 1100 °C as shown in Table 4 and Fig. 8.

Conventional ingot casting. As shown in Fig. 7, upon cooling the steel to 1450 °C, MnS began to precipitate and their amount increase sharply up to 0.05 g for all temperatures.

Due to lower solubility of oxygen, hydrogen and nitrogen in steel and their increase interaction with silicon, the hydrogen and nitrogen based micro segregation will form. H_6SiO_7 begin to grow at 1550 °C and its amount keep increasing until 1450 °C. Similarly, the NH_4HS-based precipitates form at 1450 °C and keep increasing. However, H_4SiO_4 began to nucleate at 1800 °C, but it gets disappear below 1450 °C. As per studies, the area around inclusion is the preferred site for hydrogen accumulation, so as to escape hydrogen from steel surface and diffuse in the steel. The oxide region inside inclusion, promotes the concentration of hydrogen aggregation at the interface. Moreover, these hydrogen enriched inclusions be crack initiation sites during service (Peng *et al*., 2021; Garet *et al*., 1998).

VAR treated ingot. As shown in Fig. 8, due to low pressure treatment at 0.01 torr, very little amount of

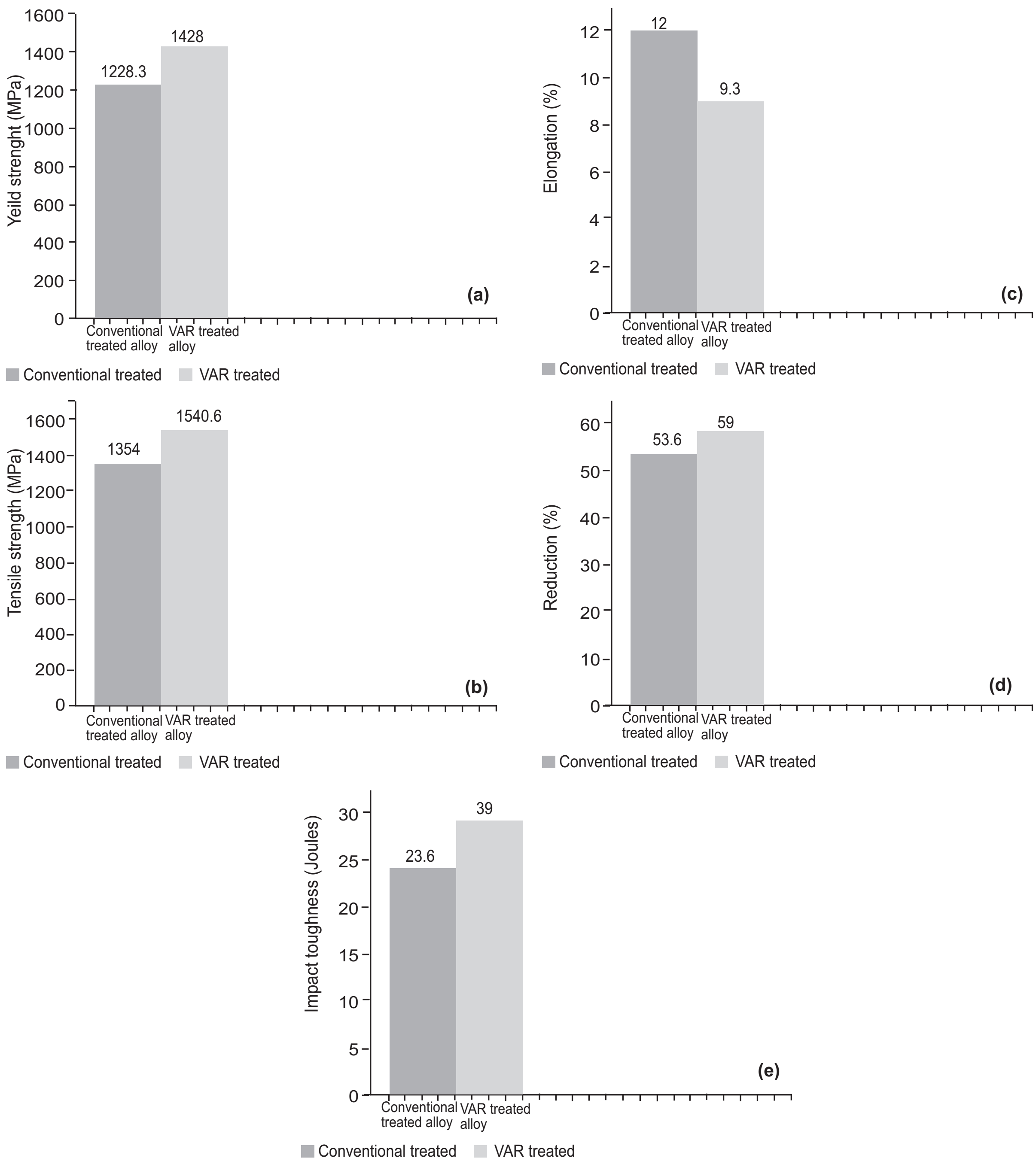

Fig. 6. The mechanical properties of conventionally treated and VAR treated ingots, (**a**)Yield strength, (**b**) Tensile strength, (**c**) % Elongation, (**d**) % Reduction and (**e**) Impact strength.

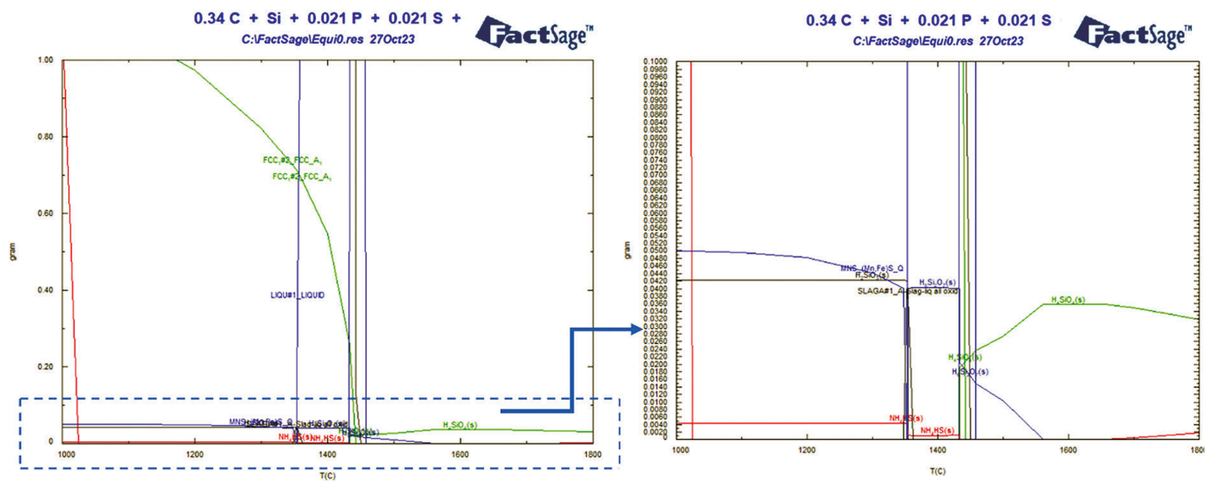

Fig. 7. The thermodynamic calculations based on equilibrium for inclusions during solidification of conventional treated steel.

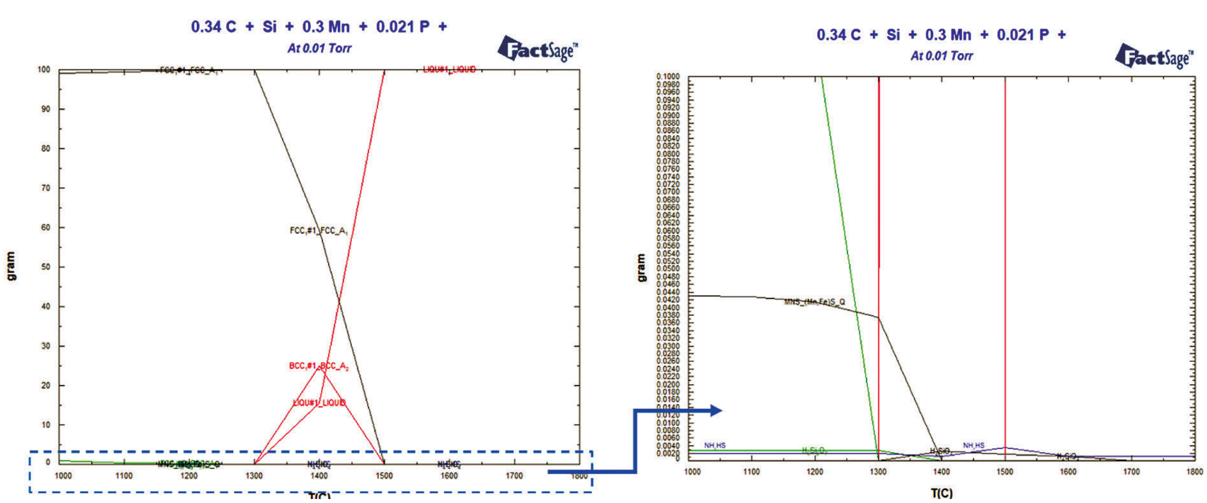

Fig. 8. The thermodynamic calculations based on equilibrium for inclusions during solidification of VAR treated steel.

micro segregation forms as compare to conventional route. Below 1200 °C, cementite began to form and keep increases in amount up to 4 g at 1000 °C. Moreover, 0.2 g of MnS and 0.05 g of SiO_2 form below 1200 °C. The MnS containing iron and silicon rich inclusions are the preferred sites for hydrogen trapping (Garet *et al*., 1998).

Conclusions

In this study, the ingots of H13 tool steel were produced using two routes *i.e*., conventional and VAR treated. Since non-metallic inclusions are of major concern that can imparts mechanical properties in service conditions. Hence, dissatisfaction among various consumers is of major concern. In order to overcome this problem, the ingots were made in extremely low pressure about 0.01 torr. This low pressure will subsequently decrease the level of gas entrapment and hence non-metallic inclusions. The absence of inclusions allowed for better impact toughness along with greater yield strength. High yield strength is certainly a crucial requirement for dies used in forming operations. A decrease in the level of NMI index for oxides, sulfides and silicates types of inclusions with and without vacuum treatment was investigated.

The higher hydrogen, nitrogen and oxygen content *i.e.*, 1.5 ppm, 249 ppm and 26 ppm respectively are responsible to produce oxides, sulfides and silicates-based inclusions with hydrogen and nitrogen trapping were observed with both thin and thick morphologies in case of conventional ingot casting. However, a very little number of inclusions were found for VAR treated ingots. The thermodynamic equilibrium calculations were compared with experimental results. On the basis of this comparison, inclusion types and their amount can be predicted well.

Although producing H13 through ingot casting has been a traditional and viable process route, it also has its downsides due to which there is a general dissatisfaction among various consumers regarding low performance. All these issues mainly arise due to the higher non-metallic inclusion content. Producing the grade under extremely low pressures can definitely resolve this issue.

The whole idea of the study was based on the fact that H13 shall be produced by controlling the harmful factors in the very early stages (by introducing vacuum) of its production rather than carrying out later post production adjustments, in order to produce H13 that could outperform the conventionally cast version.

Acknowledgment

The authors are thankful to the technical staff of the QAD department of Peoples Steel Mills Limited and more especially to Engr. Muhammad Kamran Bhatti for his technical support throughout this work and also, grateful to the Department of Materials Engineering for providing this opportunity.

Conflict of Interest. The authors declare that they have no conflict of interest.

References

ASTM, 2022. Standard Test Methods for Notched Bar Impact Testing of Metallic Materials (E23-24), *Annual Book of ASTM Standards*, pp. 3-4, P.O. Box C700, West Conshohocken, USA. https://doi.org/10.1520/E0023-22

Avner, S.H. 1974. *Introduction to Physical Metallurgy*, 386 pp., 2nd ed., McGraw-Hill, New York, USA.

Bahrami, A., Anijdan, S.M., Golozar, M., Shamanian, M., Varahram, N. 2005. Effects of conventional heat treatment on wear resistance of AISI H13 tool steel. *Wear*, **258:** 846-851.

Bale, C.W., Bélisle, E., Chartrand, P., Decterov, S., Eriksson, G., Hack, K., Pelton, A. 2009. FactSage thermochemical software and databases—recent developments. *Calphad*, **33:** 295-311.

Bielefeldt, W., Vilela, A. 2010. Computational thermodynamic study of inclusions formation in the continuous casting of SAE 8620 steel. *Steel Research International*, **81:** 1064-1069.

Campbell, J. 2023. A future for vacuum arc remelting and electroslag remelting—a critical perspective. *Metals*, **13:** 1634. https://www.mdpi. com/2075-4701/13/10/1634

CINDAS LLC, 2008. High performance alloys database, H13. West Lafayette, IN, USA.

Cyril, N., Fatemi, A., Cryderman, B. 2009. Effects of sulfur level and anisotropy of sulfide inclusions on tensile, impact and fatigue properties of SAE 4140 steel. *SAE International Journal of Materials and Manufacturing*, **1:** 218-227.

Davis, J.R. 1995. *ASM Specialty Handbook: Tool Materials*, 501 pp., ASM International, Material Park, USA.

Deo, B., Boom, R. 1993. Primary steelmaking metallurgy: slag formation. In: *Proceeding of Fundamentals of Steelmaking Metallurgy*, 1st ed., pp. 161-189, Prentice Hall International, UK.

Dorsch, C.J., Pinnow, K.E., Stasko, W. 1995. Martensitic Hot Work Tool Steel Die Block Article and Method of Manufacture, US Patent No.5447800A, 5th September, 1995.

Ferrari, M.C., Andersson, J., Kvarnström, M. 2013. Influence of lowered austenitisation temperature during hardening on tempering resistance of modified H13 tool steel (*Uddeholm Dievar*). *International Heat Treatment and Surface Engineering*, **7:** 129-132.

Garet, M., Brass, A., Haut, C., Guttierez-Solana, F. 1998. Hydrogen trapping on non metallic inclusions in Cr-Mo low alloy steels. *Corrosion Science*, **40:** 1073-1086.

Ghosh, A. 2009. Mathematical model for prediction of composition of inclusions formed during solidification of liquid steel. *ISIJ International*, **49:** 1819-1827.

Guanghua, Y., Xinmin, H., Yanqing, W., Xingguo, Q., Ming, Y., Zuoming, C., Kang, J. 2010. Effects of heat treatment on mechanical properties of H13 steel. *Metal Science and Heat Treatment*, **52:** 393-395.

Haupt, M., Vadenbo, C., Zeltner, C., Hellweg, S. 2017. Influence of input-scrap quality on the environmental impact of secondary steel production. *Journal of Industrial Ecology*, **21:** 391-401.

Huang, Y., Cheng, G., Li, S., Dai, W. 2019. Precipitation behavior of large primary carbides in cast H13 steel. *Steel Research International*, **90:** 1900035.

Huang, K., Liu, Q. 1996. Blowhole formation during solidification of liquid steel. *Steel Research*, **67:** 268-272.

Li, B., Zhang, S., Hu, R., Zhang, X. 2020. Dislocation density and grain size evolution in hard machining of H13 steel: numerical and experimental investigation. *Journal of Materials Research and Technology*, **9:** 4241-4254.

Ma, D.-S., Zhou, J., Chen, Z.-Z., Zhang, Z.-K., Chen, Q.-A., Li, D.-H. 2009. Influence of thermal homogenization treatment on structure and impact toughness of H13 ESR steel. *Journal of Iron and Steel Research International*, **16:** 56-60.

Maciejewski, J. 2015. The effects of sulfide inclusions on mechanical properties and failures of steel components. *Journal of Failure Analysis and Prevention*, **15:** 169-178.

Mao, W.-W., Ning, A.-G., Guo, H.-J. 2016. Nanoscale precipitates and comprehensive strengthening mechanism in AISI H13 steel. *International Journal of Minerals, Metallurgy and Materials*, **23:** 1056-1064.

Mebarki, N., Delagnes, D., Lamesle, P., Delmas, F., Levaillant, C. 2004. Relationship between microstructure and mechanical properties of a 5% Cr tempered martensitic tool steel. *Materials Science and Engineering: A*, **387:** 171-175.

Medvedeva, A., Bergström, J., Gunnarsson, S., Andersson, J. 2009. High-temperature properties and microstructural stability of hot-work tool steels. *Materials Science and Engineering*, **523:** 39-46.

Mertens, R., Vrancken, B., Holmstock, N., Kinds, Y., Kruth, J.-P., Van Humbeeck, J. 2016. Influence of powder bed preheating on microstructure and mechanical properties of H13 tool steel SLM parts. *Physics Procedia*, **83:** 882-890.

Ning, A., Mao, W., Chen, X., Guo, H., Guo, J. 2017. Precipitation behavior of carbides in H13 hot work die steel and its strengthening during tempering. *Metals*, **7:** 70.

Nordgren, A., Melander, A. 1989. Deformation behaviour of different types of inclusion during chip formation in turning of quenched and tempered steels. *Materials Science and Technology*, **5:** 940-951.

Olson, G., Lieberman, D., Saxena, A., 2013. In: *Proceedings of International Conference on Martensitic Transformations* (ICOMAT 2008), pp. 179-185, June 29–July 4, 2008. Hoboken, NJ: John Wiley & Sons, Santa Fe, New Mexico, USA.

Pan, Y.-T., Chen, C.-Y., Wang, S. 2016. Development of H13 ESR hot work tool steels produced using continuous casting electrodes. *China Steel Technical Report*, **29:** 49-55.

Pauliuk, S., Milford, R.L., Muller, D.B., Allwood, J.M. 2013. The steel scrap age. *Environmental Science and Technology*, **47:** 3448-3454.

Peaslee, K., Singh, V., Lekakh, S. 2011. Inclusion Engineering for Improved Properties in Steel Castings. In: *Proceedings of the Richard J. Fruehan Symposium*, pp. 1-9, USA.

Peng, Z., Liu, J., Huang, F., Zhang, S., Hu, Q., Wang, Z., Wang, Y. 2021. The significance of inclusion morphology and composition in governing hydrogen transportation and trapping in steels. *International Journal of Hydrogen Energy*, **46:** 28811-28822.

Qamar, S., Sheikh, A.K., Arif, A., Pervez, T., Siddiqui, R. 2007. Heat treatment of a hot-work die steel. *Archives of Materials Science and Engineering*, **28:** 503-508.

Ragnarsson, L. 2010. Formation of non-metallic inclusions and the possibility of their removal during ingot casting. *Ph.D. Thesis*, 57 pp., KTH Royal Institute of Technology, Stockholm, Sweden.

Ragnarsson, L., Sichen, D. 2010. Inclusions generated during ingot casting of tool steel. *Steel Research International*, **81:** 40-47.

Samuel, F. 1983. Interrelations of microstructure, mechanical properties and fracture behaviour in a Cr-Mo steel. *Transactions of the Iron and Steel Institute of Japan*, **23:** 646-651.

Smoljan, B. 2009. An analysis of relationships between behavior and microstructure constitution of hot-work tool steel. *Materials and Manufacturing Processes*, **24:** 786-790.

Song, M., Nzotta, M., Sichen, D. 2011. Effect of ladle slag of previous heat on number of non-metallic inclusions in ladle treatment of tool steel.

Ironmaking and Steelmaking, **38:** 584-589.

Thornton, P. 1971. The influence of nonmetallic inclusions on the mechanical properties of steel: a review. *Journal of Materials Science*, **6:** 347-356.

Tomita, Y. 1995. Effect of morphology of nonmetallic inclusions on tensile properties of quenched and tempered 0.4 C-Cr-Mo-Ni steel. *Materials Characterization*, **34:** 121-128.

Totten, G.E. 2006. Steel Heat Treatment: Metallurgy and Technologies, 221-222 pp., CRC press, Boca Raton, Florida.

Van Ende, M.-A., Guo, M., Zinngrebe, E., Blanpain, B., Jung, I.-H. 2013. Evolution of non-metallic inclusions in secondary steelmaking: Learning from inclusion size distributions. *ISIJ International*, **53:** 1974-1982.

Waudby, P.E. 1973. The Formation of Non-metallic Inclusions During Steelmaking. *Ph.D. Thesis*, 326 pp., Sheffield Hallam University, UK.

Wayman, C.M. 1964. *Introduction to the Crystallography of Martensitic Transformations*, 1st ed., 193 pp., Macmillan Series in Materials Science, New York, USA.

Wu, L., Liu, K., Mei, H., Bao, G., Zhou, Y., Wang, H. 2022. Thermodynamics analysis and pilot study of reusing medium and high alloy steel scrap using induction melting and electroslag remelting process. *Metals*, **12:** 944.

Zhong, P. 2007. Effect of tempering temperature on microstructure and mechanical properties in new-type ultrahigh strength steel. *Journal of Iron and Steel Research International*, **14:** 288-291.

Zhu, J., Lin, G., Zhang, Z., Xie, J. 2020. The martensitic crystallography and strengthening mechanisms of ultra-high strength rare earth H13 steel. *Materials Science and Engineering: A*, **797:** 140139.